RESEARCH ARTICLE

Cerebellum Dysfunction in Patients With *PRRT2*-Related Paroxysmal Dyskinesia

Asya Ekmen, MD, Aurelie Meneret, MD, PhD, Romain Valabregue, PhD, Benoit Beranger, BSc, Yulia Worbe, MD, PhD, Jean-Charles Lamy, PhD, Sofien Mehdi, BTech, Anais Herve, RN, Isaac Adanyeguh, PhD, Gizem Temiz, BSc, Philippe Damier, MD, PhD, Domitille Gras, MD, PhD, Agathe Roubertie, MD, PhD, Juliette Piard, MD, PhD, Vincent Navarro, MD, PhD, Eugenie Mutez, MD, PhD, Florence Riant, MD, PhD, Quentin Welniarz, PhD, Marie Vidailhet, MD, PhD, Stephane Lehericy, MD, PhD, Sabine Meunier, MD, PhD, Cecile Gallea, PhD,* and Emmanuel Roze, MD, PhD*

Correspondence
Dr. Gallea
cecile.gallea.icm@gmail.com

Neurology® 2022;98:e1077-e1089. doi:10.1212/WNL.0000000000200060

Abstract

Background and Objectives

The main culprit gene for paroxysmal kinesigenic dyskinesia, characterized by brief and recurrent attacks of involuntary movements, is *PRRT2*. The location of the primary dysfunction associated with paroxysmal dyskinesia remains a matter of debate and may vary depending on the etiology. While striatal dysfunction has often been implicated in these patients, evidence from preclinical models indicates that the cerebellum could also play a role. We aimed to investigate the role of the cerebellum in the pathogenesis of *PRRT2*-related dyskinesia in humans.

Methods

We enrolled 22 consecutive right-handed patients with paroxysmal kinesigenic dyskinesia with a pathogenic variant of *PRRT2* and their matched controls. Participants underwent a multimodal neuroimaging protocol. We recorded anatomic and diffusion-weighted MRI, as well as resting-state fMRI, during which we tested the aftereffects of sham and repetitive transcranial magnetic stimulation applied to the cerebellum on endogenous brain activity. We quantified the structural integrity of gray matter using voxel-based morphometry, the structural integrity of white matter using fixel-based analysis, and the strength and direction of functional cerebellar connections using spectral dynamic causal modeling.

Results

Patients with *PRRT2* had decreased gray matter volume in the cerebellar lobule VI and in the medial prefrontal cortex, microstructural alterations of white matter in the cerebellum and along the tracts connecting the cerebellum to the striatum and the cortical motor areas, and dysfunction of cerebellar motor pathways to the striatum and the cortical motor areas, as well as abnormal communication between the associative cerebellum (Crus I) and the medial prefrontal cortex. Cerebellar stimulation modulated communication within the motor and associative cerebellar networks and tended to restore this communication to the level observed in healthy controls.

Discussion

Patients with *PRRT2*-related dyskinesia have converging structural alterations of the motor cerebellum and related pathways with a dysfunction of cerebellar output toward the cerebello-thalamo-striato-cortical network. We hypothesize that abnormal cerebellar output is the primary dysfunction in patients with a *PRRT2* pathogenic variant, resulting in striatal dysregulation and paroxysmal dyskinesia. More broadly, striatal dysfunction in paroxysmal dyskinesia might be secondary to aberrant cerebellar output transmitted by thalamic relays in certain disorders.

RELATED ARTICLE

Editorial
No Neuron Operates in Isolation
Page 389

*These authors contributed equally to this work as senior authors.

From Sorbonne Université (A.E., A.M., R.V., B.B., Y.W., J.-C.L., S.M., A.H., I.A., G.T., V.N., Q.W., M.V., S.L., S.M., C.G., E.R.), INSERM, CNRS, Paris Brain Institute; APHP Hôpital de La Pitié Salpêtrière (A.M., V.N., M.V., S.L., E.R.), Assistance Publique des Hôpitaux de Paris, Sorbonne Université, France; Center for Magnetic Resonance Research (I.A.), University of Minnesota, Minneapolis; University of Nantes (P.D.), CHU Nantes, CIC 1314; Hôpital Robert-Debré (D.G.), Paris; INM (A.R.), Université de Montpellier, INSERM, CHU Montpellier, Département de Neuropédiatrie; Integrative and Cognitive Neurosciences Research (Unit EA481) (J.P.), Centre de génétique humaine, Université de Franche-Comté, Besançon; Université de Lille (E.M.), Inserm, CHU Lille, U1172-LilNCog-Lille Neuroscience and Cognition; and Service de Génétique Moléculaire (F.R.), Hôpital Saint-Louis, Assistance Publique des Hôpitaux de Paris, France.

Go to Neurology.org/N for full disclosures. Funding information and disclosures deemed relevant by the authors, if any, are provided at the end of the article.

Glossary

cTBS = continuous theta burst stimulation; **CTM** = cerebello-thalamo-motor cortex; **CTP** = cerebello-thalamo-prefrontal; **CTS** = cerebello-thalamo-striatal; **DCM** = dynamic causal modeling; **DMN** = default mode network; **FC** = fiber-bundle cross section; **FD** = fiber density; **FDI** = first dorsal interosseous; **FOD** = fiber orientation distribution; **GMV** = gray matter volume; **MNI** = Montreal Neurological Institute; **mPFC** = medial prefrontal cortex; **MT** = motor threshold; **PKD** = paroxysmal kinesigenic dyskinesia; **rsfMRI** = resting-state fMRI; **TMS** = transcranial magnetic stimulation; **VBM** = voxel-based morphometry.

Trial Registration Information:

ClinicalTrials.gov identifier: NCT03481491.

Paroxysmal kinesigenic dyskinesia (PKD) is characterized by brief and recurrent attacks of dystonia or other involuntary movements, typically triggered by sudden voluntary movements.[1] Monoallelic variations of the *PRRT2* gene (HGNC: 30,500) account for up to 90% of familial cases of PKD and half of the sporadic cases, depending on the population.[2,3]

The location of the primary dysfunction resulting in paroxysmal dyskinesia remains a question of debate and may vary depending on the etiology. The respective roles of the striatum and the cerebellum in its pathogenesis are likely critical.[4] For example, paroxysmal dyskinesia associated with GTP cyclohydrolase I deficiency is probably caused by the reduction in dopamine levels in the striatal microcircuitry,[5] and lesions of the globus pallidus internus, the main output of the basal ganglia receiving input from striatal projection neurons, can also result in paroxysmal dyskinesia.[6] Likewise, bilateral pallidal stimulation can improve paroxysmal dyskinesia in some patients.[7,8] Conversely, converging preclinical evidence indicates that cerebellar dysfunction plays a key role in paroxysmal dyskinesia associated with *ATP1A3* variations.[9-11]

Patients with *PRRT2* monoallelic variations rarely display episodic ataxia,[3,12,13] whereas patients with biallelic variations can have cerebellar atrophy and often experience prolonged episodes of cerebellar ataxia.[14,15] In keeping with these observations, the highest levels of *PRRT2* expression have been found in the cerebellar granule cells.[16,17] Specific suppression of *PRRT2* in these granule cells was sufficient to induce dyskinesia in mice.[18] While previous neuroimaging studies in patients with PKD have found anatomic or functional abnormalities in the basal ganglia, the thalamus and motor cortical regions, and the prefrontal cortex, the cerebellum is yet to be investigated.[19,20]

Here, we investigated the possibility that cerebellar dysfunction plays a critical role in the pathogenesis of *PRRT2*-related PKD. To this end, we combined a comprehensive anatomic and functional neuroimaging approach and transcranial magnetic stimulations (TMSs) of the cerebellum in a cohort of 22 patients with *PRRT2*-related PKD and 22 matched healthy controls.

Methods

Population

We enrolled 22 consecutive right-handed patients with PKD with a pathogenic variant of *PRRT2* and 22 healthy controls (HCs) matched for age and sex. We collected the patients' history and demographic, genetic, and clinical information. Patients with active epilepsy or a history of stroke were excluded. HCs were recruited from the database of the Pitié-Salpetrière Clinical Investigation Center (Paris, France). The patients were recruited through the French dystonia network.

Standard Protocol Approvals, Registrations, and Patient Consents

Before data collection, the full protocol was approved by the Regional Ethics Committee "Comité de Protection des Personnes Sud-Méditerranée" (reference 17.060) and was registered on ClinicalTrials.gov (NCT03481491). In accordance with the Declaration of Helsinki, written informed consent was obtained from all participants (or guardians of participants) in the study (consent for research).

Organization of the Protocol

Both the HCs and patients were investigated during 2 visits on 2 consecutive days: the first was an anatomic MRI session, and the second was a resting-state fMRI (rsfMRI) session interleaved with cerebellar TMS (continuous theta burst stimulation [cTBS]). Baseline rsfMRI data were first acquired before application of sham cerebellar TMS followed immediately by postsham rsfMRI acquisition. After a pause of 30 minutes, the patients underwent real cerebellar TMS followed immediately by post-cTBS fMRI acquisition. Between the cerebellar stimulations and MRI recordings, the participants were moved from the neighboring stimulation room to the MRI room on a nonmagnetic wheelchair to minimize muscular activity.

Data Acquisition

Patients treated for PKD with antiepileptics (n = 11) discontinued their treatment at least 1 week before the MRI session. MRIs were acquired with a 3T Siemens PRISMA

system (Siemens, Erlangen, Germany) with a 32-channel head-neck coil at the Neuroimaging Research Center of the Paris Brain Institute.

Anatomic MRI

During the first visit, we acquired a 3-dimensional T1-weighted image (magnetization-prepared rapid gradient-echo) with the following characteristics: voxel size 1 × 1 × 1 mm^3, field of view 256 × 256 × 176 mm^3, repetition time 6.172 seconds, echo time 3 milliseconds, and flip angle 90°. We also acquired diffusion-weighted images (echo-planar imaging 2-dimensional) with the following characteristics: spatial resolution 1.7 × 1.7 × 1.7 mm^3; b factor 2,000, 1,000, and 300 s/mm^2; gradient directions 60, 32, and 8; dimensions 118 × 118 × 81 mm^3; echo-planar imaging factor 128; repetition time 3.5 seconds; echo time 75 milliseconds; and flip angle 90°. The gradient directions were interleaved with 4 non–diffusion-weighted reference images (b0 images, b value = 0 s/mm^2). Another b0 image with an opposite phase-encoding blip was acquired to correct image distortions due to individual susceptibilities.

Functional MRI

During the second visit, we acquired functional resting-state images using a 9-minute multiecho multiband echo-planar imaging pulse sequence (2.5-mm isotropic resolution; 54 slices; repetition time/echo time 1,600/15.2, 37.17, and 59.14 milliseconds; multiband 3; iPAT 2; flip angle 73°; field of view 84 × 84 mm^2; pixel bandwidth 2,125 Hz). The participants were instructed to close their eyes, to remain still during the scan, and not to fall asleep. Their heart and respiratory rates were recorded by a digital sensor and a belt and were used later to remove physiologic noise from the blood oxygen level–dependent signal. Each participant underwent 3 resting-state acquisitions (baseline, after sham, after cTBS).

Transcranial Magnetic Stimulation

During the second visit, the participants were moved to the adjoining TMS room immediately after the baseline recordings. The intensity of the cerebellum stimulation was set according to the motor threshold (MT) for the right first dorsal interosseous (FDI) muscle.[21] To calculate the MT_{FDI}, the TMS pulses were applied over the left motor cortex with a 70-mm figure-of-eight coil connected to a magnetic stimulator (Magstim Company Ltd, Whitland, UK). For repetitive TMS, the cerebellar lobule VIII was targeted with a neuronavigation system. The TMS coil was placed according to standard procedures (eAppendix 1, links.lww.com/WNL/B765) and maintained over this target during the 40-second stimulation period. A 70-mm figure-of-eight cooled coil connected to a SuperRapid^2 magnetic stimulator (Magstim Company Ltd) was used to deliver the repetitive stimulation to the right cerebellum (ipsilateral to the dominant hand). The sham cerebellar stimulation applied after baseline recordings consisted of 600 stimuli delivered at 10% of the MT in 3-pulse bursts at 50 Hz repeated every 200 milliseconds.[22] Such stimulation does not modulate the cerebellar output.[23] After the 30-minute pause that followed the postsham resting-state acquisition, the participants were moved back to the stimulation room for cTBS, consisting of 600 stimuli delivered at 85% of the MT in 3-pulse bursts at 50 Hz repeated every 200 milliseconds.[22] Such stimulation can modulate the cerebellar output for at least 30 minutes.[23] The stimulation intensities were in accordance with the limit recommended by the current guidelines for delivering repeated TMS.[24] After having undergone all the TMS procedures, the participants were asked, "Which of the 2 TMS sessions did you think was the real stimulation?"

Data Analysis

Population

Statistics were calculated with Matlab (MATLAB, version 2017b, MathWorks Inc, Natick, MA). Demographic parameters (age, sex, and education level in total years of education starting from primary school) were compared between the groups with 2-sample *t* tests. Answers to the TMS questionnaire were entered in a vector of 22 values for each group. Because binary responses have a 50% chance of being randomly correct, we compared the 22 values of each group to a random vector composed of 1 and 0 values (MATLAB function rand, 50% of 1 or 0 values) using a 2-sample *t* test.

Anatomic T1

We applied voxel-based morphometry (VBM) using the VBM8 toolbox[25] to compare regional gray matter differences between patients and HCs. Data preprocessing was performed following the standard VBM8 pipeline, with normalization of gray matter images in the Montreal Neurological Institute (MNI) template space using Dartel. Nonlinear modulation of normalized gray matter images was used to correct for individual brain sizes. Smoothing was applied with an 8-mm full width half-maximum gaussian kernel. All statistical designs included age, sex, and total intracranial volume as nuisance regressors. We used a 2-sample *t*-test to evaluate gray matter group differences and a multiple regression analysis with disease duration and age at onset as covariables of interest to investigate the association of clinical parameters with gray matter maps. Results were thresholded at $p \leq 0.05$ using probabilistic threshold-free cluster enhancement with family-wise error correction across the whole brain.

Diffusion MRI

Using fixel-based analysis, we investigated white matter fiber density (FD; reflecting intra-axonal volume) and fiber-bundle cross section (FC; the area occupied by the axons).[26] The term fixel here refers to the image unit, similar to a voxel but containing information about individual fiber orientation. Motion, bias field correction, and global intensity normalization of the diffusion-weighted images were individually performed (eAppendix 1, links.lww.com/WNL/B765). Fiber orientation distributions (FODs) were computed with constrained spherical deconvolution. The FODs were then used to create a study template to register all the individual FOD images into a

common space. FD was estimated by nonparametric numeric integration with a dense sampling of the FOD. In addition, we estimated a fixel-specific measure based on morphology differences in the plane perpendicular to the fixel direction and compared this measure across participants to investigate variations in local FC. We compared measures of FD and FC in all white matter fixels across both groups using a general linear model, including age, sex, and total intracranial volume as nuisance covariates. Connectivity-based smoothing and statistical inference were performed with connectivity-based fixel enhancement using 2 million streamlines and default parameters (smoothing = 10-mm full width half-maximum, C = 0.5, E = 2, H = 3). Family-wise error–corrected *p* values were assigned to each fixel by nonparametric permutation testing with 5,000 permutations. To better assess all the fiber pathways affected, we reconstructed the pathways that passed through regions of local structural alterations using the whole-brain template-derived tractogram.

Functional MRI

Definition of Regions of Interest

After preprocessing to combine the multiple echoes and denoise and normalize the data to the MNI template space, we conducted an independent component analysis at the level of the group to identify regions of interest (GIFT software, version 3.0[27]) using 20 components (eAppendix 1, links.lww.com/WNL/B765). The cerebello-thalamo-striatal (CTS) loop comprised the cerebellum (cerebellar lobule VI and VIII separately), the central medial nuclei of the thalamus, and the sensorimotor striatum (posterior dorsal putamen). The cerebello-thalamo-motor cortex (CTM) loop comprises the cerebellum, the ventral intermediate nuclei of the thalamus, the primary sensorimotor cortex, and the supplementary motor area. Because functional abnormalities have previously been observed in the thalamus and medial prefrontal cortex (mPFC),[19] we tested whether these abnormalities could be related to aberrant cerebellar influence. We looked at the cerebellar Crus I that is anatomically connected to the prefrontal cortex through the medial dorsal thalamic nucleus, which we labeled the cerebello-thalamo-prefrontal (CTP) loop. Last, we examined the default mode network (DMN) comprising the posterior cingulate cortex, the mPFC, and the bilateral inferior parietal lobule.

Dynamic Causal Modeling

The spectral dynamic causal modeling (DCM) analyses were conducted with DCM12 implemented in SPM12 (revision 12.2). This method is more advantageous than conventional models (1) to isolate group differences in connectivity parameters due to greater consistency and (2) to evaluate connectivity differences across independent sessions.[28] DCM models were specified for each network (eAppendix 1, links.lww.com/WNL/B765) as a fully connected model. Using spectral DCM,[29] we obtained individual measures of causal interactions between regions, as well as the amplitude of endogenous neuronal fluctuations within each region.[29] We reported group and stimulation effects using the equivalent of a global linear model in the DCM framework[30] with age and sex as covariates of nuisance. We evaluated (1) the average connectivity across participants in each group, (2) the between-group comparison (patients with *PRRT2* vs HC), and (3) the between-session comparison for the *PRRT2* group (after sham vs after cTBS). We report only effects (i.e., changes in directed connectivity) that have a posterior probability >0.95, according to the bayesian statistical framework.

Data Availability

Anonymized data not published within this article will be made available on request from any qualified investigator if approved by the Internal Review Board. In their current status, the data are considered to be the intellectual property of the Paris Brain Institute and INSERM.

Results

Population

Patients' characteristics are summarized in Table 1. Twelve of the 22 HCs (55%) and 11 of the 22 patients (50%) gave the correct answer to the question about which 1 of the 2 sessions was the real stimulation. Neither group identified the sham from the real stimulation at a higher probability than chance (patients with *PRRT2* $p = 0.74$, HCs $p = 0.54$).

Voxel-Based Morphometry

Gray matter volume (GMV) was lower in the bilateral cerebellar lobule VI and the right mPFC of the patients compared to the HCs (Figure 1A and Table 2). Reverse contrast failed to reveal any difference. Disease duration correlated with the bilateral cerebellum Crus II only: patients with longer disease duration had a lower GMV in Crus II (eFigure 1, A and B, links.lww.com/WNL/B765). Age at onset correlated with GMV in the bilateral cerebellum Crus I and the left cerebellar lobule VI and in the bilateral sensorimotor striatum: patients with an earlier age at onset of PKD had a lower GMV in these 2 areas (Figure 1, B and C and eFigure 1, C and D).

Diffusion MRI

The patients had focal microstructural fiber abnormalities with changes in both within-voxel FD (Figure 2) and FC (eFigure 2, links.lww.com/WNL/B765), both of which were increased compared with the HCs. For FC, group differences were maximal in the motor lobule VI of the cerebellum and the mPFC. For FD, group differences were located at the proximal portion of the superior cerebellar peduncles, in the middle cerebellar peduncles, and in the posterior limb of the internal capsule.

Structural alterations in the patients were located in areas intersecting the outgoing and incoming cerebellar pathways (Figure 3). Many of the fiber pathways that connected to the affected cerebellar regions showed a significant increase in FD. On the basis of the anatomico-functional characteristics

Table 1 Demographic and Clinical Characteristics of Patients With *PRRT2* and HCs

Characteristics	Patients with *PRRT2* (n = 22)	HCs (n = 22)	*p* Value[a]
Age, y	29.4 (±12.2)	30.6 (±11.7)	0.74
Age range, y	15–49	19–54	
Sex, F/M, n	8/14	8/14	
Education, total y from primary school	14.0 (±3.7)	15.4 (±2.3)	0.12
Mutation (c.649dupC/other), n	22/0		
Age at onset, y	9.1 (±3.2)		
Disease duration, y	17.2 (±10.6)		
Family history (yes/no), n	18/4		
Dyskinesia type (dystonia/chorea/ballism), n	22/0/0		
Attack duration (<15/<30/60 s), n	7/9/6		
Attack frequency (monthly)	15.0 (±15.4)		
Attack localization (focal/unilateral/bilateral), n	1/1/20		
Facial involvement (yes/no), n	5/17		
Treatment (yes/no), n	11/11		
Medication (CBZ/LTG/LEV), n	8/2/1		
Prognosis (good/bad), n	22/0		

Abbreviations: CBZ = carbamazepine; HC = healthy control; LEV = levetiracetam; LTG = lamotrigine.
Patients with *PRRT2* and healthy controls did not differ in age, sex, or educational level. Quantitative data are expressed as mean (±SD).
[a] Two-tailed 2-sample *t* test.

of these tracts, we identified outgoing fibers from the cerebello-thalamo-striato-cortical tract, incoming fibers from the cortico-cerebellar tract encompassing the middle cerebellar peduncle, and cortico-spinal tract encompassing the posterior regions of the internal capsule.

Functional MRI

Regions of Interest

The CTM, CTS, CTP, and DMN independent components were identified by the spatial independent component analysis (eFigure 3 and eTable 1, links.lww.com/WNL/B765). The spheres centered on the peaks (CTM, CTS, CTP) or on a priori coordinates (DMN) were used for further DCM analyses (Figure 4; coordinates given in eAppendix 1).

Dynamic Causal Modeling

DCM group analysis showed that the patients had a dysfunction of cerebellar outputs within the CTS, CTM, and CTP loops (Figure 5A). According to the mathematical sense, negative coupling parameters are associated with anti-correlated responses (inhibitory connections) between 2 nodes, whereas positive coupling parameters are associated with correlated response (facilitatory connections) between 2 nodes.[31] For the CTS and CTM loops, the patients had decreased inhibition from the cerebellar lobule VIII to the thalamic relays. In contrast, the connection from the cerebellar lobule VI to the thalamic relays was less facilitated in the patients than in the HCs. Connections from the thalamic relays to the striatum (facilitated in patients and inhibited in HCs) and primary sensorimotor cortex (less inhibited in patients) were also disrupted. For the CTS, cerebellar dysfunction in the patients was accompanied by increased self-inhibition in the cerebellar lobule VI, cerebellar lobule VIII, and sensorimotor striatum. Self-inhibition was unchanged for cortical motor areas. In addition to the cerebellar and striatal dysfunctions of the motor circuits, we observed a difference in connectivity in the DMN, accompanied by a decrease in self-inhibition (self-facilitation) in the mPFC.

Continuous TBS modulation of the cerebellum tended to restore thalamo-cortical connectivity toward the level observed in the HCs: connections from the thalamic relays to the striatum and from the thalamic relays to the primary sensorimotor cortex were less facilitated in the patients after cTBS (Figure 5B). In the CTS, cTBS decreased self-inhibition of the cerebellar lobule VIII (target of the stimulation) and the sensorimotor striatum.

Discussion

We show that patients with *PRRT2*-related PKD have converging structural alterations of the motor cerebellum and

Figure 1 GMV Abnormalities in Patients With *PRRT2*

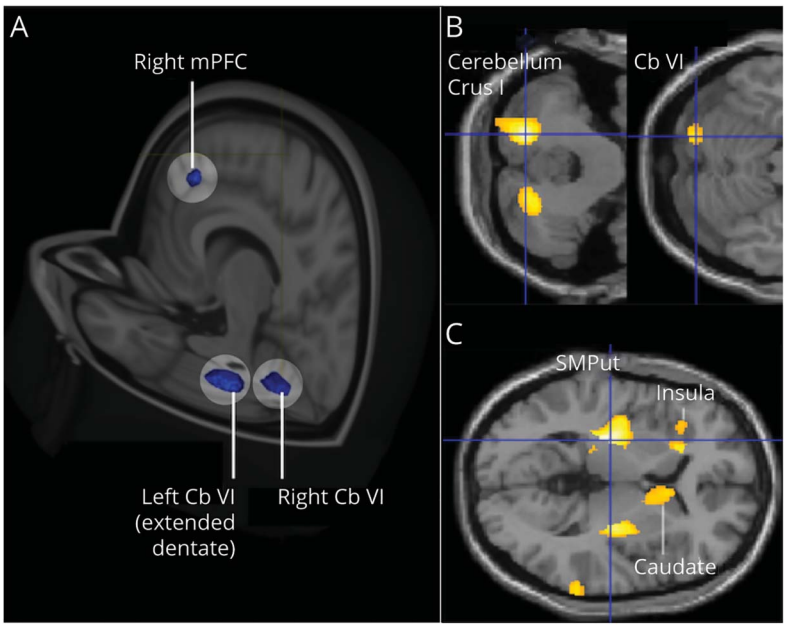

(A) Results of the 2-sample *t* test comparing gray matter volume (GMV) between patients with *PRRT2*-related paroxysmal kinesigenic dyskinesia and healthy controls (HCs). Main clusters showing a group difference are displayed on a 3-dimensional render; $p < 0.001$ threshold-free cluster enhancement correction. (B and C) Results of the multiple regression analysis showing the GMV correlation with age at disease onset ($p < 0.001$). Corresponding coordinates of peak changes are given in Table 2. CbVI = cerebellar lobule VI; mPFC = medial prefrontal cortex; SMCaud = caudate sensorimotor territory of caudate; SPM = statistical parametric mapping; SMPut = sensorimotor territory of putamen; VBM = voxel-based morphometry.

related pathways with a dysfunction of cerebellar output toward the cerebello-thalamo-striato-cortical network. From these findings and previous preclinical evidence, we suggest that abnormal cerebellar output is the primary dysfunction resulting in PKD in patients with a variation of *PRRT2*. More broadly speaking, striatal dysfunction in paroxysmal dyskinesia might be secondary to aberrant cerebellar output transmitted to the striatum in certain disorders such as *PRRT2*-related PKD.

The main strengths of our study lie in the homogeneity of the patient group (comprised exclusively of patients diagnosed with PKD with a pathogenic variant in *PRRT2*) and the use of a cutting-edge multimodal imaging approach. Furthermore, our study was original in that we focused on cerebellar dysfunction, a concept supported by several very recent preclinical experiments.[16-18,32] However, a few limitations deserve to be mentioned. First, some of our patients with PKD were on long-term treatment, comprising mainly low-dose carbamazepine. Hence, although highly unlikely, we cannot formally rule out that the long-term treatment had an influence on our structural findings. Second, all patients with PKD included in the study had the same c.649dupC pathogenic variant of the *PRRT2* gene, a variant that is implicated in ≈75% of patients with *PRRT2*-related PKD and that leads to a premature stop codon. Nevertheless, it is thought that all the variants of this gene linked to PKD result in similar gene haploinsufficiency with a subsequent protein loss of function.[33] It is thus likely that the effect of the variation is representative of the *PRRT2*-PKD patient population and that this aspect does not interfere with the generalizability of our findings. Another potential limitation is that we did not randomize the order of the sham and active TMS sessions. The reason was that our

Table 2 Results of the Group Difference of GMV (VBM)

Anatomic localization of clusters	MNI coordinates of global maxima	Cluster size, n voxels	Statistics (*z* score)
Reference = AAL atlas	x, y, z		
HC > *PRRT2*			
L cerebellum (lobule VI, dentate)	−15, −60, −26	350	3.65
R mPFC (superior frontal gyrus)	15, 66, 4	156	3.63
R ACC	8, 44, 24	145	3.49
R cerebellum (lobule VI, dentate)	10, −60, −26	127	3.35

Abbreviations: AAL = automated anatomic labeling; ACC = anterior cingulate cortex; GMV = gray matter volume; HC = healthy controls; MNI = Montreal Neurological Institute; mPFC = medial prefrontal cortex; VBM = voxel-based morphometry.

Figure 2 Fixel-Based Analysis Comparing White Matter Structure in Patients With PRRT2-PKD and HCs

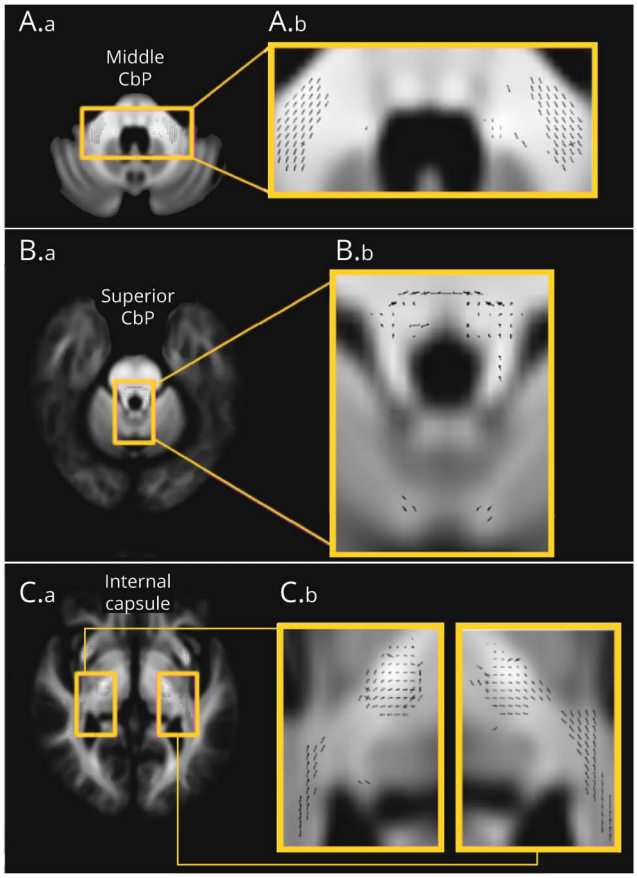

Fixels with a significant ($p < 0.05$) increase in fiber density in patients with PRRT2-related paroxysmal kinesigenic dyskinesia (PKD) compared to healthy controls (HCs). Yellow frames show the areas of interest with fixel abnormalities, which are enlarged on the right. Fixels that are displayed show significant group difference with family-wise error–corrected *p* values and overlaid on the total voxel-wise group template. All significant differences are displayed by a black fixel. Fixel-based analysis enables fiber tract–specific inference by attributing *p* values to each fixel in voxels containing multiple fiber populations. (A) Axial view of the cerebellum (A.a), enlarged at the level of the middle cerebellar peduncule (CbP) (A.b). (B) Axial view of the cerebellum (B.a), enlarged at the level of the superior CbP (B.b). (C) Axial view of the cerebrum (C.a), enlarged at the level of the internal capsule (C.b).

protocol could not last >2 days, preventing us from measuring the effect of cerebellar TMS with a double-blind procedure and a sufficient washout period (typically 1 week). However, from the debriefing question, none of the patients (or HCs) who were naive to TMS could decipher the real from the sham stimulation.

Whole-brain voxel-based analysis of the gray matter found a decrease in the (motor) lobule VI of the cerebellum. GMV in the cerebellar areas correlated with clinical characteristics. Patients with PKD onset at an early age had a lower GMV in the left cerebellar lobule VI and bilateral cerebellar Crus I. Patients with longer disease duration had a lower GMV in cerebellar Crus II. These results suggest a link between the cerebellum and the pathogenesis of the disease.

We found microstructural alterations in the patients located at the proximal portion of the superior cerebellar peduncles (conveying cerebellar efferents), in the middle cerebellar peduncles (conveying cerebellar afferents from the brain structures), and in the posterior limb of the internal capsule (conveying corticospinal tract fibers). Fixel-based analysis is a novel framework that provides fiber specific information to quantify white matter characteristics without anatomic a priori, unlike seed-to-target analysis. In our patients, the apparent FD was greater in the superior cerebellar peduncles, likely reflecting a larger number of axons in that fiber population or the presence of bigger axons.[26] In addition, FC was greater in the motor cerebellum (lobule VI) and the mPFC. This may account for an increase in the spatial extent occupied by the white matter fibers due to abnormal axonal growth or an overexpansion of cerebellar outputs.[26] These changes in tissue microstructure can modify the capacity of the fiber bundle to relay information in the cerebellum. Moreover, microstructural alterations were found in posterior regions of the internal capsule. These tracts connect primary sensorimotor regions, as well as the parietal lobe to the spinal cord.[34] The contributions from the sensory areas terminate in the sensory nuclei of the brainstem and spinal cord (which are below the field of view of the diffusion-weighted imaging data), where they modulate sensory transmission. This might suggest that sensory information is processed differently in patients with *PRRT2*-PKD compared to HCs.

Three studies have investigated structural abnormalities in patients with PKD using other techniques. Two of them used graph theory applied on structural covariance of GMV[35] and white matter properties[36] but did not include the cerebellum in the construction of the morphologic network used in the analyses. The remaining study investigated the basal ganglia and found a decrease in GMV and white matter abnormalities in the medial thalamus in patients with PKD.[37] Furthermore, another study, using seed-to-target analyses, found increased structural connectivity in the thalamo-cortical motor tract in patients with PKD.[38] Our results indicate that structural connectivity was also altered between the cerebellum and the thalamic relay, upstream of the thalamo-cortical tract.

Using spectral DCM, we found a reduction in the information flow from the motor cerebellar lobule VI to the thalamic relay and an altered drive of the thalamic relay toward the striatum and the primary motor cortex (Figure 5C), probably resulting in a modification of the balance between the striatal and motor cortex activity. This finding is consistent with microstructural white matter abnormalities of the cerebellar outputs, indicating abnormal axonal growth or an overexpansion of cerebellar outputs. A previous resting-state study of 11 patients with PKD of unknown genetic cause found an increased interhemispheric functional connectivity in the basal ganglia-thalamo-cortical network and the cerebellum.[39] Similar changes in the connectivity pattern in the cerebello-thalamo-striato-cortical network have been modeled in dopa-induced dyskinesia of Parkinson disease.[40,41] Although

Figure 3 Identification of White Matter Pathways Carrying Microstructural Abnormalities in Patients With PRRT2-PKD on Fixel-Based Analysis

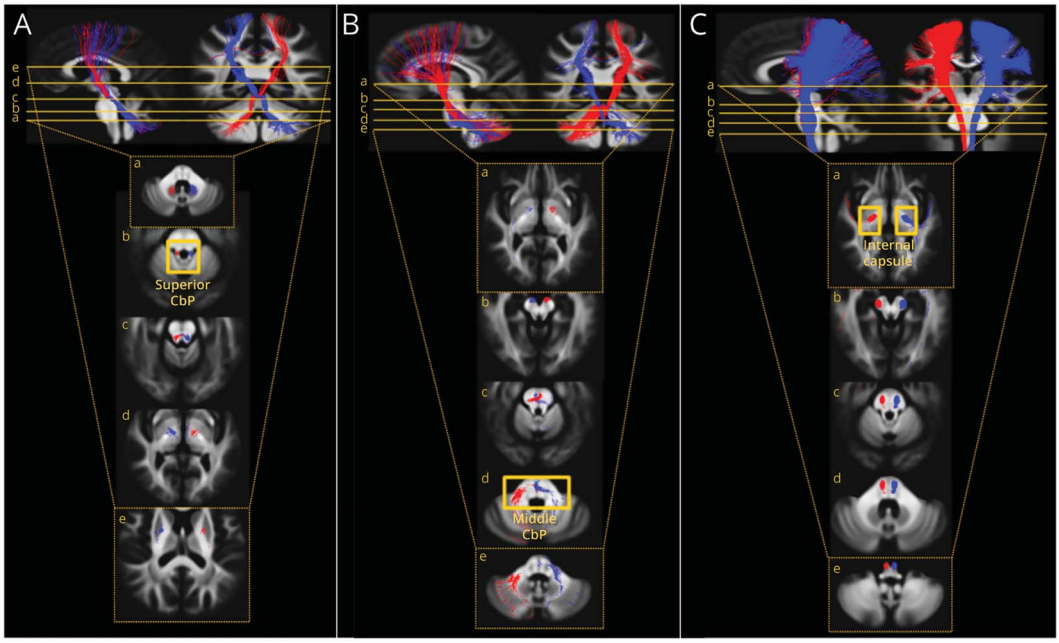

The figure shows streamlines that pass through white matter fixels with a significant increase in fiber density comparing patients with *PRRT2*-related paroxysmal kinesigenic dyskinesia (PKD) and healthy controls (yellow frames in Figure 2). Tracts passing through these regions are superimposed on the sagittal (top left) and coronal (top right) views of the fiber density template. Multiple axial views are displayed to appreciate the trajectory of the tracts. These tracts were filtered from the whole-brain tractography (red tracts are connecting the right brain hemisphere; blue tracts are connecting the left brain hemisphere). (A) Cerebello-thalamo-striato-cortical tract passing through the superior cerebellar peduncles (CbPs) (outgoing cerebellar tract). Axial views are at the level of cerebellar dentate nucleus (A.a), superior CbP (A.b), midbrain (A.c), thalamus (A.d), and striatum A.(e). (B) Cortico-ponto-cerebellar tract passing through the CbP (incoming cerebellar tract). Axial views are at the level of the striatum (B.a), anterior bundle of the mesencephalon (B.b), decussation of the cerebellar tract (B.c), middle CbPs (B.d), and cerebellar hemispheres (B.e). (C) Cortico-spinal tract passing through the internal capsule. Axial views are at the level of posterior part of the internal capsule (C.a), lateral part of the anterior bundle of the mesencephalon (C.b), upper pons (C.c), lower pons (C.d), and anterior bundle of the upper spinal cord (C.e). For each view (axial, coronal, and sagittal), a single 2-dimensional slice of fixels is shown and overlaid on the group template.

Parkinson disease dyskinesia and PKD constitute 2 different clinical and pathophysiologic paradigms, they share similarities, namely episodic hyperkinetic movements associated with striatal dysfunction. Of note, in our patients with *PRRT2*-PKD, the thalamic drive was altered to a greater extent toward the striatum than toward the primary motor cortex. This highlights the importance of cerebello-striatal pathway dysfunction in explaining PKD pathophysiology.

In addition to the communication between nodes, our DCM approach investigated another class of connectivity parameters: self-inhibitory or intrinsic connections. Intrinsic connections reflect how sensitive a region is to afferent inputs. A reduction in intrinsic connections is thus a vector of internal instability. We observed a decrease in self-inhibition in cerebellar and striatal nodes in our patients with *PRRT2*-PKD, suggesting internal instability of the motor cerebellum and motor striatum. TMS-induced modulation of cerebellar output tended to restore cerebellar self-inhibition and thalamo-striatal and thalamo-cortical motor connectivity. This fits with the fact that modulation of cerebellar drive can change corticostriatal plasticity[42] and can affect thalamo-cortical[23] or cortico-cortical coupling.[43] The type of stimulation we used induced a decrease of the inhibitory input of the cerebellar cortex onto the dentate. This would eventually lead to a facilitation of glutamatergic connections between the dentate and the thalamus and between the thalamus and cortical motor areas.

Our study provides further evidence of mPFC dysfunction in patients with *PRRT2*-PKD. More specifically, we found an increase in self-inhibition in the prefrontal node, dysregulated connectivity from the thalamus to the prefrontal cortex, and a decrease in GMV of medial prefrontal areas. Previous studies have also found structural alterations of the medial prefrontal area.[19,38] In addition, our results show that mPFC connectivity is modified by an alteration of the cerebellar drive on thalamic relay, leading to an enhanced excitatory coupling between the thalamic relay and the mPFC. A study involving 8 patients with *PRRT2*-related PKD found decreased functional connectivity between the thalamus and the prefrontal cortex compared to PKD patients without *PRRT2* variations and controls.[38] Furthermore, cerebellar TMS restored thalamo-prefrontal connectivity and affected prefrontal cortex sensitivity to inputs (decrease in self-inhibition). This indicates that the cerebellum can influence prefrontal activity in

Figure 4 Regions of Interest for Resting-State Connectivity Defined From the Independent Component Analysis

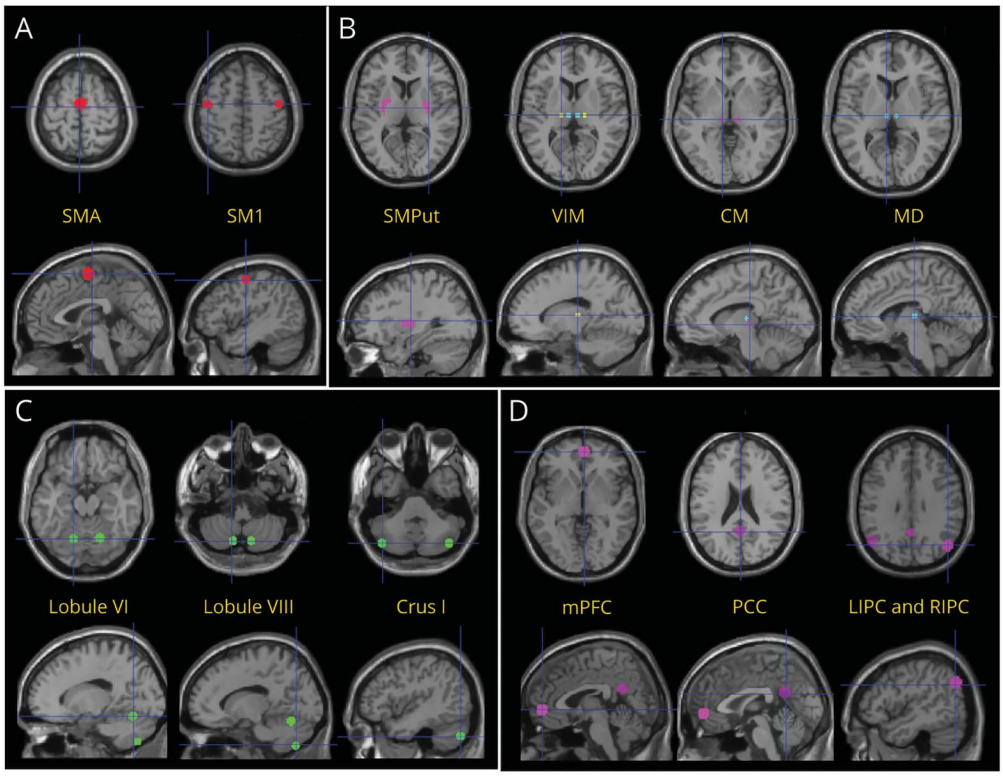

Regions of interest of the cerebellar loops and default mode network (DMN) defined as spheres from the components shown in eFigure 3, links.lww.com/WNL/B765. (A) Cortical motor areas: supplementary motor area (SMA) and primary sensorimotor cortex (SM1). (B) Subcortical areas: sensorimotor territory of putamen (SMPut), ventral-intermediate nucleus of the thalamus (VIM), central-medial nucleus of the thalamus (CM), and medial-dorsal nucleus of the thalamus (MD). (C) Cerebellar areas: cerebellar lobule VI, cerebellar lobule VIII, and cerebellar Crus I. (D) Cortical areas of the DMN: medial prefrontal cortex (mPFC), posterior cingulate cortex (PCC), and left (LIPC) and right (RIPC) inferior parietal cortex.

patients with *PRRT2*-related PKD. Reciprocal anatomic loops exist between the cerebellum and the medial prefrontal cerebral cortex.[44] The prefrontal cortex receives substantial input from thalamic regions, including the zone of termination of cerebellar afferents.[45] In addition, we found that connectivity in the default brain network, including the medial prefrontal area, was disrupted (Figure 5A). This shows that dysfunction of the mPFC could be explained by, or be associated with, dysfunction of cerebral cortical nodes in addition to the cerebellum. An interesting point is that modulation of prefrontal activity with repetitive TMS can influence functional connectivity between the mPFC and the striatum.[46] This suggests that dysfunction of the striatum and the mPFC could be linked in a positive loop gain as a Larsen effect (i.e., self-amplified activity). We think that the disorder of the prefrontal network might link the classic triggering factors of *PRRT2*-PKD and the role of this network in anticipating outcomes and shifting attention.[45]

Various preclinical evidence supports the role of the cerebellum in the pathogenesis of *PRRT2*-related PKD. The highest level of *PRRT2* expression is found in the cerebellum (granule cell and molecular layers) with the RNA transcript located exclusively within the granule cells of the cerebellar cortex.[16,17] Granule cells in *PRRT2* knockout mice had an increased intrinsic excitability with abnormal sodium currents.[32] *PRRT2* knockout mice recapitulating the human PKD phenotype had a higher excitatory strength of the synapses at the parallel fibers between granule cells and Purkinje cells during high-frequency stimulation.[16] Specific suppression of *PRRT2* in the granule cells (but not the cortex or the striatum) in the mice was sufficient to bring about heat-induced dyskinesia associated with abnormal firing of the Purkinje cells.[18] Together, these experiments demonstrate abnormal excitability of the granule cells (expressing *PRRT2*) that induces synaptic dysfunction between the granule and Purkinje cells within the molecular layer.[16-18,32] This synaptic dysfunction likely results in a disruption of the normal inhibitory control of the Purkinje cells on deep cerebellar nuclei, which eventually transmit the final excitatory output from the cerebellum to the thalamus and related subcortical and cortical motor networks. Our findings, together with data from animal models and human experiments, provide converging evidence that the cerebellum is the primary location of the disorder and that subsequent dysfunction of the CTS network causes *PRRT2*-PKD.

Likewise, paroxysmal dystonic episodes linked to variations in the *ATP1A3* gene are associated with altered cerebellar activity,

Figure 5 Resting-State Connectivity Estimates of the Group Analysis Using Spectral Dynamic Causal Modeling

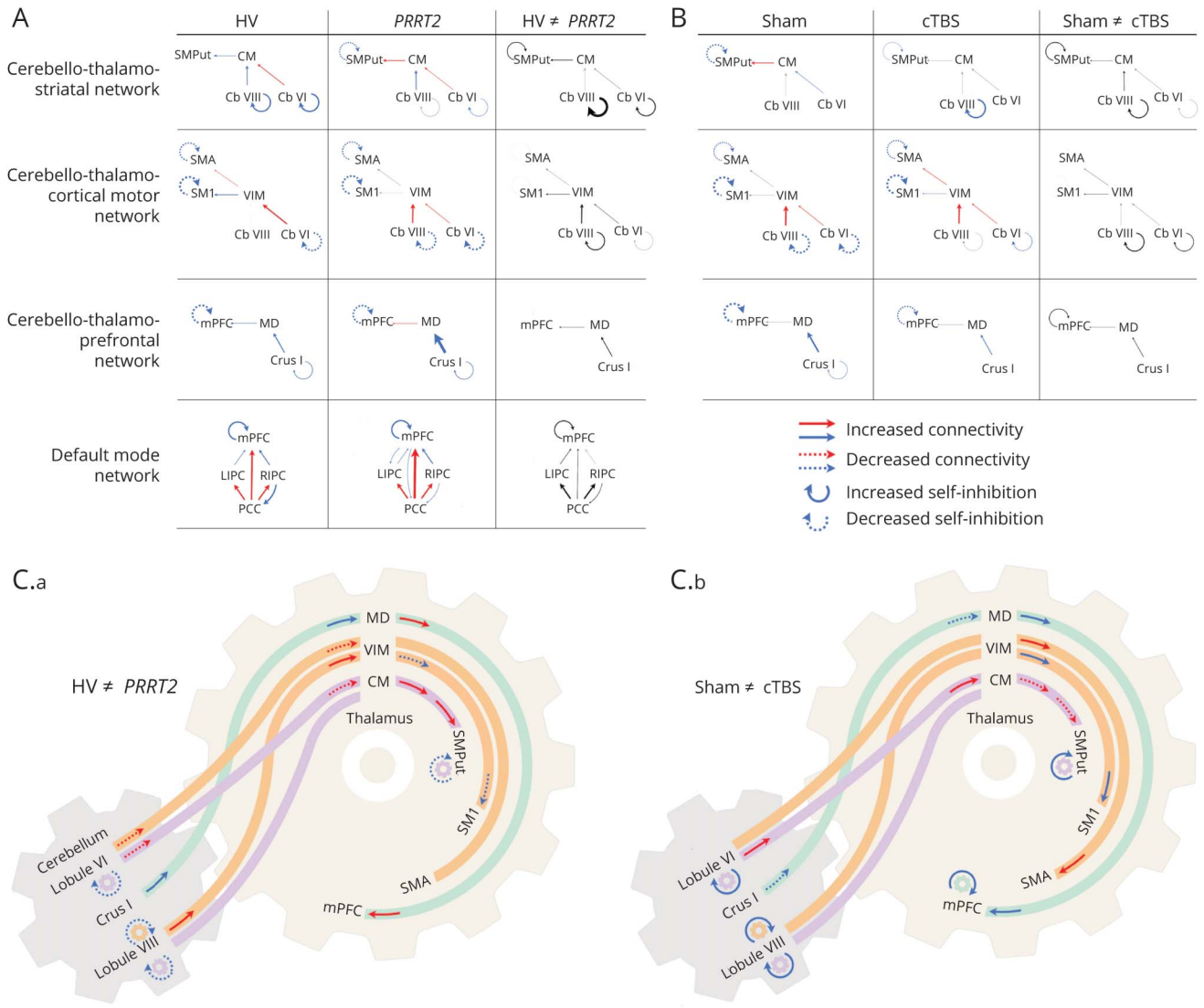

Cerebellar networks include cerebellar regions of the right hemisphere and cerebral regions of the left hemisphere. (A) Results of the comparison between healthy controls (HCs) and patients with *PRRT2* at baseline. Networks of interest are displayed in lines; within- (HC, *PRRT2*) and between- (HV ≠ *PRRT2*) group results are displayed in columns. (B) Results of the comparison between the session after cerebellar sham stimulation and the session after cerebellar real stimulation (continuous theta burst stimulation [cTBS]) in patients with *PRRT2*. Networks of interest are displayed in lines; within- (sham, cTBS) and between- (sham ≠ cTBS) session results are displayed in columns. Posterior estimates for each connection (exact values in eTables 2–5, links.lww.com/WNL/B765) are represented by arrows (only for the posterior expectations of connections within 95% CIs). Within-group results represent the commonalities between the bayesian parameter averages of each session (A for baseline, B for postsham and post-cTBS). Self-connections (within region) are displayed with circular arrows; extrinsic (between regions) connections are displayed with straight arrows. Arrows are in red when positive or in blue when negative for within-group results, in black in case of a significant difference, and in gray in case of a nonsignificant difference for the group analyses. Thickness of the arrow indicates the connection strength. (C) Simplified schema of dynamic causal modeling extrinsic and self-connections that are different between groups (C.a) or modulated by cerebellar transcranial magnetic stimulation in patients with *PRRT2* (C.b); red shows positive and blue shows negative; only significant differences are displayed. CbVI = Cerebellum lobule VI; Cb VIII = Cerebellum lobule VIII; CM = central-medial nucleus of the thalamus; Crus I = cerebellar Crus I; LIPC = left inferior parietal cortex; MD = medial-dorsal nucleus of the thalamus; mPFC = medial prefrontal cortex; PCC = posterior cingulate cortex; RIPC = right inferior parietal cortex; SMA = supplementary motor area; SM1 = primary sensorimotor cortex; SMPut = putamen, sensorimotor territory; VIM = ventral-intermediate nucleus of the thalamus.

which is transmitted to the deep cerebellar nuclei.[9-11] Selective lesions of these nuclei or their thalamic relay, as well as drug-induced cerebellar inhibition, can alleviate dystonic episodes in animal models of the disease. Tottering mice have dystonic attacks associated with a maladaptive plasticity involving upregulation of calcium channels in the cerebellum, and degeneration of the Purkinje cells stops the dystonic episodes in these mice.[47] Similarly, removal of the cerebellum eliminates paroxysmal episodes in lethargic mice carrying a variation in the *CCHB4* gene.[48] Rodents and nonhuman primates have a disynaptic pathway linking cerebellar nuclei to the striatum that is critical for motor control.[42,49,50] We hypothesize that paroxysmal dystonia/dyskinesia is a network disorder characterized mainly by striatal dysfunction that could be either primary or secondary to aberrant cerebellar output transmitted to the striatum, as in *PRRT2*- or ATP1A3-related paroxysmal

dyskinesia. Cerebellar dysfunction could also influence the final motor output without incorporating the striatum, especially through the cerebellar projection on the various motor areas after a thalamic relay, the motor areas being the main origin of the corticospinal tract.

Acknowledgment

The authors thank the patients, their families, and their doctors for their participation and help. They also thank the Center for Clinical Investigations (Pitié Neurosciences 1422, Hôpital de la Pitié-Salpêtrière, Paris, France) and the platform TMS and CENIR (Institut du Cerveau, Paris, France) for their invaluable support with the acquisitions. They thank Isabelle Dusart for her scientific advice that was helpful in writing the manuscript. They also thank Felicity Neilson for her language editing services.

Study Funding

This work received financial support from Association des malades atteints de dystonie and from Fondation pour la Recherche Médicale (prix Line-Pomaret, grant attributed to A.E.). This project was also supported by Agence Nationale de la Recherche under the frame of the European Joint Programme on Rare Diseases (ANR-16-CE37-0003-03). In addition, this project received funding from the European Union's Horizon 2020 research and innovation programme under the EJP RD COFUND-EJP N° 825,575 - EurDyscover.

Disclosure

The authors report no disclosures relevant to the manuscript. Go to Neurology.org/N for full disclosures.

Publication History

Received by *Neurology* June 1, 2021. Accepted in final form January 3, 2022.

Appendix Authors

Name	Location	Contribution
Asya Ekmen, MD	Sorbonne Université, INSERM, CNRS, Paris Brain Institute, France	Drafting/revision of the manuscript for content, including medical writing for content; major role in the acquisition of data; analysis or interpretation
Aurelie Meneret, MD, PhD	Sorbonne Université, INSERM, CNRS, Paris Brain Institute, France; APHP Hôpital de La Pitié Salpêtrière, Assistance Publique des Hôpitaux de Paris, Sorbonne Université, France	Drafting/revision of the manuscript for content, including medical writing for content; major role in the acquisition of data
Romain Valabregue, PhD	Sorbonne Université, INSERM, CNRS, Paris Brain Institute, France	Drafting/revision of the manuscript for content, including medical writing for content; analysis or interpretation
Benoit Beranger, BSc	Sorbonne Université, INSERM, CNRS, Paris Brain Institute, France	Study concept or design; analysis or interpretation
Yulia Worbe, MD, PhD	Sorbonne Université, INSERM, CNRS, Paris Brain Institute, France	Drafting/revision of the manuscript for content, including medical writing for content; analysis or interpretation
Jean-Charles Lamy, PhD	Sorbonne Université, INSERM, CNRS, Paris Brain Institute, France	Drafting/revision of the manuscript for content, including medical writing for content; major role in the acquisition of data
Sofien Mehdi, BTech	Sorbonne Université, INSERM, CNRS, Paris Brain Institute, France	Drafting/revision of the manuscript for content, including medical writing for content; major role in the acquisition of data
Anais Herve, RN	Sorbonne Université, INSERM, CNRS, Paris Brain Institute, France	Drafting/revision of the manuscript for content, including medical writing for content; major role in the acquisition of data
Isaac Adanyeguh, PhD	Sorbonne Université, INSERM, CNRS, Paris Brain Institute, France; Center for Magnetic Resonance Research, University of Minnesota, Minneapolis	Drafting/revision of the manuscript for content, including medical writing for content; analysis or interpretation
Gizem Temiz, BSc	Sorbonne Université, INSERM, CNRS, Paris Brain Institute, France	Drafting/revision of the manuscript for content, including medical writing for content; analysis or interpretation
Philippe Damier, MD, PhD	University of Nantes, CHU Nantes, CIC 1314, France	Drafting/revision of the manuscript for content, including medical writing for content; major role in the acquisition of data
Domitille Gras, MD, PhD	Hôpital Robert-Debré, Paris, France	Drafting/revision of the manuscript for content, including medical writing for content; major role in the acquisition of data
Agathe Roubertie, MD, PhD	INM, Université de Montpellier, INSERM, CHU Montpellier, Département de Neuropédiatrie, France	Drafting/revision of the manuscript for content, including medical writing for content; major role in the acquisition of data
Juliette Piard, MD, PhD	Integrative and Cognitive Neurosciences Research (Unit EA481), Centre de génétique humaine, Université de Franche-Comté, Besançon, France	Drafting/revision of the manuscript for content, including medical writing for content; major role in the acquisition of data
Vincent Navarro, MD, PhD	Sorbonne Université, INSERM, CNRS, Paris Brain Institute, France; APHP Hôpital de La Pitié Salpêtrière, Assistance Publique des Hôpitaux de Paris, Sorbonne Université, France	Drafting/revision of the manuscript for content, including medical writing for content; major role in the acquisition of data

Continued

Appendix *(continued)*

Name	Location	Contribution
Eugenie Mutez, MD, PhD	Univ. Lille, Inserm, CHU Lille, U1172-LilNCog-Lille Neuroscience and Cognition, France	Drafting/revision of the manuscript for content, including medical writing for content; major role in the acquisition of data
Florence Riant, MD, PhD	Service de Génétique Moléculaire, Hôpital Saint-Louis, Assistance Publique des Hôpitaux de Paris, France	Drafting/revision of the manuscript for content, including medical writing for content; major role in the acquisition of data
Quentin Welniarz, PhD	Sorbonne Université, INSERM, CNRS, Paris Brain Institute, France	Drafting/revision of the manuscript for content, including medical writing for content; analysis or interpretation
Marie Vidailhet, MD, PhD	Sorbonne Université, INSERM, CNRS, Paris Brain Institute, France	Drafting/revision of the manuscript for content, including medical writing for content; study concept or design; analysis or interpretation
Stephane Lehericy, MD, PhD	Sorbonne Université, INSERM, CNRS, Paris Brain Institute, France	Drafting/revision of the manuscript for content, including medical writing for content; study concept or design; analysis or interpretation
Sabine Meunier, MD, PhD	Sorbonne Université, INSERM, CNRS, Paris Brain Institute, France	Drafting/revision of the manuscript for content, including medical writing for content; study concept or design; analysis or interpretation
Cecile Gallea, PhD	Sorbonne Université, INSERM, CNRS, Paris Brain Institute, France	Drafting/revision of the manuscript for content, including medical writing for content; major role in the acquisition of data; study concept or design; analysis or interpretation; other
Emmanuel Roze, MD, PhD	Sorbonne Université, INSERM, CNRS, Paris Brain Institute, France; APHP Hôpital de La Pitié Salpêtrière, Assistance Publique des Hôpitaux de Paris, Sorbonne Université, France	Drafting/revision of the manuscript for content, including medical writing for content; major role in the acquisition of data; study concept or design; analysis or interpretation; other

References

1. Méneret A, Roze E. Paroxysmal movement disorders: an update. *Rev Neurol (Paris).* 2016;172(8-9):433-445.
2. Chen W-J, Lin Y, Xiong Z-Q, et al. Exome sequencing identifies truncating mutations in PRRT2 that cause paroxysmal kinesigenic dyskinesia. *Nat Genet.* 2011;43(12):1252-1255.
3. Meneret A, Grabli D, Depienne C, et al. PRRT2 mutations: a major cause of paroxysmal kinesigenic dyskinesia in the European population. *Neurology.* 2012;79(2):170-174.
4. Delorme C, Giron C, Bendetowicz D, Méneret A, Mariani LL, Roze E. Current challenges in the pathophysiology, diagnosis, and treatment of paroxysmal movement disorders. *Expert Rev Neurother.* 2021;21(1):81-97.
5. Dale RC, Melchers A, Fung VSC, Grattan-Smith P, Houlden H, Earl J. Familial paroxysmal exercise-induced dystonia: atypical presentation of autosomal dominant GTP-cyclohydrolase 1 deficiency. *Dev Med Child Neurol.* 2010;52(6):583-586.
6. Friedman J, Feigenbaum A, Chuang N, Silhavy J, Gleeson JG. Pyruvate dehydrogenase complex-E2 deficiency causes paroxysmal exercise-induced dyskinesia. *Neurology.* 2017;89(22):2297-2298.
7. de Almeida Marcelino AL, Mainka T, Krause P, Poewe W, Ganos C, Kühn AA. Deep brain stimulation reduces (nocturnal) dyskinetic exacerbations in patients with ADCY5 mutation: a case series. *J Neurol.* 2020;267(12):3624-3631.
8. van Coller R, Slabbert P, Vaidyanathan J, Schutte C. Successful treatment of disabling paroxysmal nonkinesigenic dyskinesia with deep brain stimulation of the globus pallidus internus. *Stereotact Funct Neurosurg.* 2014;92(6):388-392.
9. Calderon DP, Fremont R, Kraenzlin F, Khodakhah K. The neural substrates of rapid-onset dystonia-parkinsonism. *Nat Neurosci.* 2011;14(3):357-365.
10. Fremont R, Calderon DP, Maleki S, Khodakhah K. Abnormal high-frequency burst firing of cerebellar neurons in rapid-onset dystonia-parkinsonism. *J Neurosci.* 2014;34(35):11723-11732.
11. Fremont R, Tewari A, Khodakhah K. Aberrant Purkinje cell activity is the cause of dystonia in a shRNA-based mouse model of rapid onset dystonia-parkinsonism. *Neurobiol Dis.* 2015;82:200-212.
12. Gardiner AR, Bhatia KP, Stamelou M, et al. PRRT2 gene mutations: from paroxysmal dyskinesia to episodic ataxia and hemiplegic migraine. *Neurology.* 2012;79(21):2115-2121.
13. Legris N, Chassin O, Nasser G, Riant F, Tournier-Lasserve E, Denier C. Acute-onset ataxia and transient cerebellar diffusion restriction associated with a PRRT2 mutation. *J Stroke Cerebrovasc Dis.* 2019;28(2):e3-e4.
14. Labate A, Tarantino P, Viri M, et al. Homozygous c.649dupC mutation in PRRT2 worsens the BFIS/PKD phenotype with mental retardation, episodic ataxia, and absences. *Epilepsia.* 2012;53(12):e196-199.
15. Delcourt M, Riant F, Mancini J, et al. Severe phenotypic spectrum of biallelic mutations in *PRRT2* gene. *J Neurol Neurosurg Psychiatry.* 2015;86(7):782-785.
16. Michetti C, Castroflorio E, Marchionni I, et al. The PRRT2 knockout mouse recapitulates the neurological diseases associated with PRRT2 mutations. *Neurobiol Dis.* 2017;99:66-83.
17. Calame DJ, Xiao J, Khan MM, et al. Presynaptic PRRT2 deficiency causes cerebellar dysfunction and paroxysmal kinesigenic dyskinesia. *Neuroscience.* 2020;448:272-286.
18. Tan G-H, Liu Y-Y, Wang L, et al. PRRT2 deficiency induces paroxysmal kinesigenic dyskinesia by regulating synaptic transmission in cerebellum. *Cell Res.* 2018;28(1):90-110.
19. Liu W, Xiao Y, Zheng T, Chen G. Neural mechanisms of paroxysmal kinesigenic dyskinesia: insights from neuroimaging. *J Neuroimaging.* 2021;31(2):272-276.
20. Zhang Y, Ren J, Qin Y, et al. Altered topological organization of functional brain networks in drug-naive patients with paroxysmal kinesigenic dyskinesia. *J Neurol Sci.* 2020;411:116702.
21. Rossini PM, Barker AT, Berardelli A, et al. Non-invasive electrical and magnetic stimulation of the brain, spinal cord and roots: basic principles and procedures for routine clinical application: report of an IFCN committee. *Electroencephalogr Clin Neurophysiol.* 1994;91(2):79-92.
22. Huang Y-Z, Edwards MJ, Rounis E, Bhatia KP, Rothwell JC. Theta burst stimulation of the human motor cortex. *Neuron.* 2005;45(2):201-206.
23. Popa T, Russo M, Meunier S. Long-lasting inhibition of cerebellar output. *Brain Stimulat.* 2010;3(3):161-169.
24. Rossi S, Hallett M, Rossini PM, Pascual-Leone A. Safety, ethical considerations, and application guidelines for the use of transcranial magnetic stimulation in clinical practice and research. *Clin Neurophysiol.* 2012;120(12):323-330.
25. Structural Brain Mapping Group. VBM. Accessed xxxx. dbm.neuro.uni-jena.de/vbm
26. Raffelt DA, Tournier J-D, Smith RE, et al. Investigating white matter fibre density and morphology using fixel-based analysis. *NeuroImage.* 2017;144(pt A):58-73.
27. Calhoun VD, Adali T, Stevens MC, Kiehl KA, Pekar JJ. Semi-blind ICA of fMRI: a method for utilizing hypothesis-derived time courses in a spatial ICA analysis. *NeuroImage.* 2005;25(2):527-538.
28. Park H-J, Friston KJ, Pae C, Park B, Razi A. Dynamic effective connectivity in resting state fMRI. *NeuroImage.* 2018;180:594-608.
29. Razi A, Kahan J, Rees G, Friston KJ. Construct validation of a DCM for resting state fMRI. *NeuroImage.* 2015;106:1-14.
30. Friston KJ, Litvak V, Oswal A, et al. Bayesian model reduction and empirical Bayes for group (DCM) studies. *NeuroImage.* 2016;128:413-431.
31. Friston KJ, Kahan J, Biswal B, Razi A. A DCM for resting state fMRI. *NeuroImage.* 2014;94:396-407.
32. Binda F, Valente P, Marte A, Baldelli P, Benfenati F. Increased responsiveness at the cerebellar input stage in the PRRT2 knockout model of paroxysmal kinesigenic dyskinesia. *Neurobiol Dis.* 2021;152:105275.
33. Landolfi A, Barone P, Erro R. The spectrum of PRRT2-associated disorders: update on clinical features and pathophysiology. *Front Neurol.* 2021;12:629747.
34. Rizzolatti G, Luppino G. The cortical motor system. *Neuron.* 2001;31(6):889-901.
35. Li X, Lei D, Niu R, et al. Disruption of gray matter morphological networks in patients with paroxysmal kinesigenic dyskinesia. *Hum Brain Mapp.* 2020;42(2):398-411.
36. Li L, Lei D, Suo X, et al. Brain structural connectome in relation to PRRT2 mutations in paroxysmal kinesigenic dyskinesia. *Hum Brain Mapp.* 2020;41(14):3855-3866.
37. Kim JH, Kim DW, Kim JB, Suh Sil, Koh SB. Thalamic involvement in paroxysmal kinesigenic dyskinesia: a combined structural and diffusion tensor MRI analysis. *Hum Brain Mapp.* 2015;36(4):1429-1441.
38. Long Z, Xu Q, Miao H-H, et al. Thalamocortical dysconnectivity in paroxysmal kinesigenic dyskinesia: combining functional magnetic resonance imaging and diffusion tensor imaging: thalamocortical Dysconnectivity in PKD. *Mov Disord.* 2017;32(4):592-600.
39. Ren J, Lei D, Yang T, et al. Increased interhemispheric resting-state functional connectivity in paroxysmal kinesigenic dyskinesia: a resting-state fMRI study. *J Neurol Sci.* 2015;351(1-2):93-98.

40. Caligiore D, Pezzulo G, Baldassarre G, et al. Consensus paper: towards a systems-level view of cerebellar function: the interplay between cerebellum, basal ganglia, and cortex. *Cerebellum.* 2017;16(1):203-229.
41. Kishore A, Popa T. Cerebellum in levodopa-induced dyskinesias: the unusual suspect in the motor network. *Front Neurol.* 2014;5:157.
42. Chen CH, Fremont R, Arteaga-Bracho EE, Khodakhah K. Short latency cerebellar modulation of the basal ganglia. *Nat Neurosci.* 2014;17(12):1767-1775.
43. Popa D, Spolidoro M, Proville RD, Guyon N, Belliveau L, Léna C. Functional role of the cerebellum in gamma-band synchronization of the sensory and motor cortices. *J Neurosci.* 2013;33(15):6552-6556.
44. Strick PL, Dum RP, Fiez JA. Cerebellum and nonmotor function. *Annu Rev Neurosci.* 2009; 32:413-434.
45. Middleton FA, Strick PL. Cerebellar projections to the prefrontal cortex of the primate. *J Neurosci.* 2001;21(2):700-712.
46. Popa T, Morris LS, Hunt R, et al. Modulation of resting connectivity between the mesial frontal cortex and basal ganglia. *Front Neurol.* 2019;10:587.
47. Campbell DB, North JB, Hess EJ. Tottering mouse motor dysfunction is abolished on the Purkinje cell degeneration (PCD) mutant background. *Exp Neurol.* 1999;160(1):268-278.
48. Devanagondi R, Egami K, LeDoux MS, Hess EJ, Jinnah HA. Neuroanatomical substrates for paroxysmal dyskinesia in lethargic mice. *Neurobiol Dis.* 2007;27(3):249-257.
49. Hoshi E, Tremblay L, Féger J, Carras PL, Strick PL. The cerebellum communicates with the basal ganglia. *Nat Neurosci.* 2005;8(11):1491-1493.
50. Xiao L, Bornmann C, Hatstatt-Burklé L, Scheiffele P. Regulation of striatal cells and goal-directed behavior by cerebellar outputs. *Nat Commun.* 2018;9(1):3133.